in pseudoequatorial and pseudoaxial orientations, respectively, for the C(8) and C(9) methyl groups.

The absence of a significant structural trans effect (STE) in the title compound is consistent with the lack of a formal negative charge on the coordinated sulfur atom. It has been postulated[2,40] that in these types of complexes neutral S-bonded ligands such as thioethers and disulfides generate minimal STE's, whereas anionic S-bonded ligands such as thiolates, sulfenates, and sulfinates generate marked STE's, because the anionic ligands are stronger σ donors and form stronger, shorter Co–S bonds. The hypothesis is supported by the relatively long Co–S distance in the title complex (2.260 (3) Å), which may be compared to the shorter Co–S distance (2.243 (2) Å) in the analogous thiolato complex $[(en)_2Co(SCH_2COO)]^+$.[18]

Acknowledgment. Financial support by the National Science Foundation, Grant No. CHE79-26497, is gratefully acknowledged.

Registry No. $[(en)_2Co(S(SC(CH_3)_2COOH)C(CH_3)_2COO)](ClO_4)_2 \cdot 2H_2O$, 81898-13-7; $[(en)_2Co(S(SCH_2COOH)CH_2COO)]^{2+}$, 81898-17-1; $[(en)_2Co(S(SCH(CH_3)COOH)CH(CH_3)COO)]^{2+}$, 81898-14-8; $[(en)_2Co(S(SC(CH_3)_3)CH_2COO)](ClO_4)_2$, 81898-16-0; $[(en)_2Co(S(SC(CH_3)_3)CH_2COO)]Cl_2$, 81898-18-2; $[(en)_2Co(S(SC(CH_3)_3)CH(CH_3)COO)](ClO_4)_2$, 81898-20-6; $[(en)_2Co(S(SC(CH_3)_3)C(CH_3)_2COO)](ClO_4)_2$, 81898-22-8; $[(en)_2Co(S(SC(CH_3)_3)CH_2CH_2NH_2)](ClO_4)_3$, 81898-23-9; $[(en)_2Co(S(SC(CH_3)_2COOH)CH_2COO)](ClO_4)_2$, 81898-25-1; $[(en)_2Co(S(SC(CH_3)_2COOH)CH(CH_3)COO)]ZnCl_4$, 81915-54-0; $[(en)_2Co(S(SC(CH_3)_2COOH)CH_2CH_2NH_2)](ClO_4)_3$, 81915-56-2; $[(en)_2Co(S(SCH_2CH_2OH)CH_2CH_2NH_2)]^{3+}$, 81898-26-2; $[(en)_2Co(S(SCH_2C(O)OCH_3)CH_2CH_2NH_2)]^{3+}$, 81898-27-3; $[(en)_2Co(SCH_2COO)]ClO_4$, 26743-67-9; $[(en)_2Co(SCH(CH_3)COO)]ClO_4$, 60828-75-3; $[(en)_2Co(SC(CH_3)_2COO)]ClO_4$, 68645-87-4; $[(en)_2Co(SCH_2COO)]PF_6$, 81898-28-4; $[(en)_2Co(SCH_2CH_2NH_2)](ClO_4)_2$, 40330-50-5; $[(en)_2Co(SCH_2COO)]Cl$, 54453-35-9; $HSC(CH_3)_2COOH$, 4695-31-2; $H_3COC(O)SSCH_2CH_2OH$, 30453-26-0; $H_3COC(O)SSCH_2C(O)OCH_3$, 81897-82-7; $HSCH_2CH_2OH$, 60-24-2; $HSCH(CH_3)COOH$, 79-42-5; *tert*-butylsulfenyl iodide, 25558-08-1.

Supplementary Material Available: Listings of $|F_o|$ and $|F_c|$ values (Table A), anisotropic thermal parameters (Table B), root-mean-square displacements (Table C), and perchlorate bond angles (Table D) (17 pages). Ordering information is given on any current masthead page.

Contribution from the Department of Chemistry and Radiation Laboratory, University of Notre Dame, Notre Dame, Indiana 46556

Effects of Bridging Hydrogens on Metal–Metal Bonds. 1. Geometrical Comparison of $Fe_3(\mu\text{-}H)_3(CO)_9(\mu_3\text{-}CCH_3)$, $Co_3(CO)_9(\mu_3\text{-}CCH_3)$, and Model Compounds

KWAI SAM WONG, KENNETH J. HALLER, TAMAL K. DUTTA, DANIEL M. CHIPMAN,[1] and THOMAS P. FEHLNER*

Received March 9, 1982

The solid-state structure of $Fe_3(\mu\text{-}H)_3(CO)_9(\mu_3\text{-}CCH_3)$ (II) consists of a triangular M_3 base constructed of three $Fe(CO)_3$ fragments with hydrogens symmetrically bridging the M–M edges and with a C–CH_3 fragment symmetrically capping the metal triangle. The molecule has C_{3v} symmetry, each iron being six-coordinate (three carbonyl ligands, two bridging hydrogens, and the methylidyne carbon) and the capping carbon four-coordinate (three irons and the methyl carbon). The comparison of the geometry of II with that of isoelectronic $Co_3(CO)_9(\mu_3\text{-}CCH_3)$ (I) reveals several changes that are interpreted in terms of the bridging hydrogens acting as hydride-like ligands. It is demonstrated that the geometries of main-group model compounds for I and II ($CH_3CC_3H_3$ and $CH_3CB_3H_6$) as generated by ab initio calculations reproduce the structural differences of I and II. Hence, in I and II the representation of the $Co(CO)_3$ and $Fe(CO)_3$ fragments with CH and BH provides much more than a simple, descriptive analogy of the cluster bonding. Crystals of II form in the triclinic space group $P\bar{1}$ with the following unit cell parameters: a = 7.979 (2), b = 9.478 (3), c = 12.714 (4) Å; α = 93.45 (3), β = 106.94 (3), γ = 60.79 (3)°; V = 799 Å^3; Z = 2. The X-ray structure was solved as described in the text and refined to R_1 = 0.076 and R_2 = 0.075 for 2496 independent reflections.

Alkylidynetrimetal systems such as I constitute the first

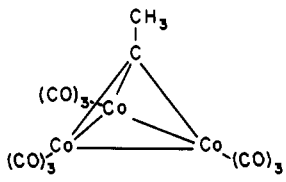

I

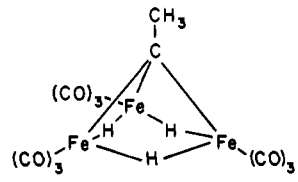

II

cluster systems to be studied systematically.[2] The geometrical structure of this cluster has been defined,[3] and synthetic routes to derivatives with a significant variation in the methylidyne carbon substituent have been developed.[4] The chemistry of the methylidyne carbon has also been elucidated, and spectroscopic and theoretical techniques have been used to define the bonding of this capping carbon to the trimetal fragment.[5] Recently, added impetus to such studies arose from the hypothesis that the μ_3-CR bonding is representative of a possible mode of binding of the CR fragment to a metal surface.[6]

(1) Radiation Laboratory.
(2) Markby, R.; Wender, I.; Friedel, R. A.; Cotton, F. A.; Sternberg, H. W. *J. Am. Chem. Soc.* **1958**, *80*, 6529.
(3) Sutton, P. W.; Dahl, L. F. *J. Am. Chem. Soc.* **1967**, *89*, 261.
(4) Seyferth, D. *Adv. Organomet. Chem.* **1976**, *14*, 97. Penfold, B. R.; Robinson, B. H. *Acc. Chem. Res.* **1973**, *6*, 73. Palyi, G.; Piacenti, F.; Marko, L. *Inorg. Chim. Acta, Rev.* **1970**, *4*, 109.
(5) Schilling, B. E. R.; Hoffmann, R. *J. Am. Chem. Soc.* **1979**, *101*, 3456. Chesky, P.; Hall, B. B. *Inorg. Chem.* **1981**, *20*, 4419. Costa, N. C. V.; Lloyd, D. R.; Brint, P.; Spalding, T. R.; Pelin, W. K. *Surf. Sci.* **1981**, *107*, L379. Costa, N. C. V.; Lloyd, D. R.; Brint, P.; Pelin, W. K.; Spalding, T. R. *J. Chem. Soc., Dalton Trans.* **1982**, 201. Wong, K. S.; Dutta, T. K.; Fehlner, T. P. *J. Organomet. Chem.* **1981**, *215*, C48. Granozzi, G.; Agnolin, S.; Casarin, M.; Osella, D. *Ibid.* **1981**, *208*, C6. Evans, J. *J. Chem. Soc., Dalton Trans.* **1980**, 1005.

0020-1669/82/1321-3197$01.25/0

Table I. Fractional Triclinic Coordinates, Anisotropic Thermal Parameters (Å²), and Isotropic Temperature Factors in $Fe_3(\mu\text{-H})_3(CO)_9(\mu_3\text{-}CCH_3)$[a]

atom	x	y	z	B_{11}	B_{22}	B_{33}	B_{12}	B_{13}	B_{23}	B,[b] Å²
Fe_1	0.1885 (1)	0.5602 (1)	0.7486 (1)	2.68 (4)	3.09 (4)	4.68 (5)	−1.13 (3)	1.30 (3)	−0.41 (3)	3.45
Fe_2	0.0857 (1)	0.8674 (1)	0.7580 (1)	3.32 (4)	3.24 (4)	5.44 (6)	−1.65 (4)	1.63 (4)	−0.20 (4)	3.74
Fe_3	−0.1124 (1)	0.7543 (1)	0.8231 (1)	3.02 (4)	3.07 (4)	5.72 (6)	−1.26 (3)	1.93 (4)	−0.17 (4)	3.64
C_{11}	0.1069 (12)	0.4157 (10)	0.7057 (7)	3.6 (3)	4.8 (3)	6.0 (4)	−1.6 (3)	2.1 (4)	−1.0 (3)	4.6
O_{11}	0.0556 (10)	0.3230 (8)	0.6795 (6)	6.5 (3)	5.7 (3)	9.9 (4)	−4.2 (2)	2.9 (3)	−2.2 (3)	6.2
C_{12}	0.4271 (13)	0.4244 (9)	0.8505 (7)	4.0 (4)	3.9 (4)	5.5 (4)	−1.7 (3)	1.3 (3)	−0.3 (3)	4.5
O_{12}	0.5769 (10)	0.3444 (8)	0.9145 (6)	4.9 (4)	6.0 (4)	7.9 (4)	−1.3 (3)	0.1 (3)	0.7 (3)	6.8
C_{13}	0.2759 (12)	0.5362 (10)	0.6316 (8)	4.2 (4)	4.6 (5)	5.6 (5)	−1.9 (3)	1.5 (3)	−0.4 (4)	4.8
O_{13}	0.3266 (11)	0.5200 (9)	0.5545 (6)	8.1 (3)	8.4 (3)	6.7 (6)	−3.7 (2)	4.3 (4)	−1.6 (3)	7.0
C_{21}	0.1757 (13)	0.8792 (9)	0.6510 (8)	4.8 (3)	3.2 (3)	7.8 (6)	−1.5 (2)	2.5 (3)	0.4 (3)	4.9
O_{21}	0.2297 (11)	0.8897 (9)	0.5784 (6)	7.6 (5)	8.8 (5)	8.5 (4)	−3.3 (4)	4.0 (4)	1.1 (3)	7.5
C_{22}	0.2588 (14)	0.9064 (11)	0.8675 (8)	5.2 (3)	5.5 (3)	6.1 (8)	−3.2 (3)	1.7 (4)	−0.5 (4)	5.3
O_{22}	0.3681 (12)	0.9281 (10)	0.9364 (7)	8.1 (3)	10.1 (4)	9.0 (4)	−6.8 (3)	1.1 (3)	−1.4 (3)	7.7
C_{23}	−0.1211 (14)	1.0704 (11)	0.7166 (8)	5.1 (4)	4.5 (3)	7.6 (4)	−2.6 (3)	3.1 (3)	−0.7 (3)	5.0
O_{23}	−0.2519 (11)	1.1991 (7)	0.6905 (7)	6.2 (4)	3.5 (4)	14.5 (4)	−0.8 (3)	3.9 (3)	1.3 (3)	6.9
C_{31}	−0.3442 (14)	0.9404 (11)	0.7898 (9)	5.0 (4)	4.0 (3)	9.8 (5)	−2.6 (3)	3.7 (4)	−1.5 (3)	5.1
O_{31}	−0.4933 (10)	1.0592 (8)	0.7674 (7)	4.5 (4)	4.3 (4)	14.1 (5)	−0.2 (4)	3.5 (4)	0.7 (3)	6.8
C_{32}	−0.0683 (14)	0.7228 (11)	0.9717 (9)	5.3 (4)	4.5 (4)	7.6 (5)	−1.7 (3)	3.3 (4)	−0.8 (3)	5.5
O_{32}	−0.0385 (13)	0.7047 (10)	1.0639 (6)	10.7 (4)	8.9 (4)	6.0 (6)	−3.5 (3)	4.2 (3)	−0.3 (4)	7.9
C_{33}	−0.2457 (12)	0.6435 (10)	0.7780 (9)	3.3 (4)	3.9 (4)	10.3 (6)	−1.4 (3)	3.1 (4)	−1.6 (4)	4.8
O_{33}	−0.3343 (10)	0.5777 (8)	0.7508 (8)	5.1 (3)	6.1 (3)	17.7 (7)	−3.7 (3)	3.8 (4)	−2.1 (4)	7.1
C	−0.0625 (11)	0.7588 (8)	0.6826 (7)	3.0 (3)	3.1 (3)	5.4 (4)	−1.1 (2)	1.1 (3)	0.1 (2)	3.8
H_3C	−0.2080 (19)	0.7957 (15)	0.5721 (10)	6.2 (6)	7.5 (6)	7.9 (7)	−1.9 (5)	2.0 (5)	0.0 (5)	7.6
H_{12}	0.265 (10)	0.697 (8)	0.803 (5)							6.5 (15)
H_{23}	0.003 (11)	0.850 (8)	0.862 (5)							4.8 (17)
H_{31}	0.137 (10)	0.564 (8)	0.852 (5)							4.2 (16)

[a] The B_{ij}'s are related to the dimensionless β_{ij}'s employed during refinement as $B_{ij} = 4\beta_{ij}/a_i^*a_j^*$. The estimated standard deviations of the least significant digits are given in parentheses. [b] The isotropic equivalents are given for the atoms that were refined anisotropically.

Alkylidynetrimetal clusters of other transition metals have been appearing more frequently of late,[7] and in a preliminary report we have described the characterization of $Fe_3(\mu\text{-H})_3(CO)_9(\mu_3\text{-}CCH_3)$ (II).[8] This compound is strictly isoelectronic to I, and its geometrical structure is analogous to that of I except that the edges of the metal triangle are bridged by hydrogens. The existence of this compound allows a direct comparison of I with II and, thus, provides a good opportunity to obtain information on the structural, electronic, and chemical roles of bridging hydrogens in metal cluster systems.

There are two limiting models for the interaction of hydrogen atoms with multinuclear transition-metal systems.[9] In one, the interstitial mode, the hydrogens simply fill in existing "holes" in the transition-metal skeleton and do not extensively perturb the geometry of the system. In the other, the ligand mode, the hydrogens act as hydridic entities exhibiting size with a tendency to achieve a characteristic M–H distance.[10] The comparison of compounds I and II provides an opportunity of exploring how the bridging hydrogens of II behave with respect to these two limiting models. Thus, here we report the complete structural determination of II and examine in detail the geometrical consequences of M–H–M interactions in a cluster system. Included is a comparison of the geometries

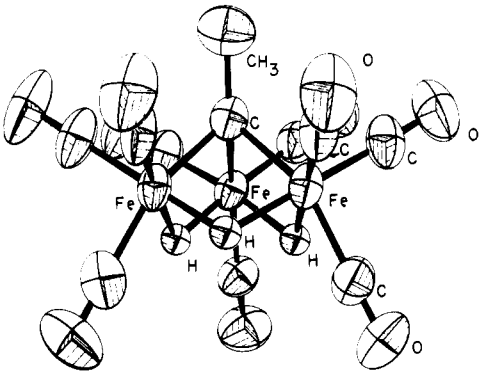

Figure 1. ORTEP view of $Fe_3(\mu\text{-H})_3(CO)_9(\mu_3\text{-}CCH_3)$ with the numbering scheme used. Atoms are represented by their thermal motion ellipsoids scaled to enclose 50% of the electron density. Hydrogen atoms on the methyl group are omitted.

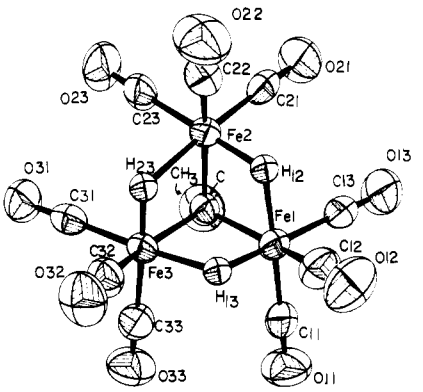

Figure 2. ORTEP view of $Fe_3(\mu\text{-H})_3(CO)_9(\mu_3\text{-}CCH_3)$ showing the threefold axis.

(6) See, for example: Muetterties, E. L.; Rhodin, T. N.; Band, E.; Brucker, C. R.; Pretzer, W. R. *Chem. Rev.* **1979**, *79*, 91. Howard, M. W.; Kettle, S. F.; Oxton, I. A.; Powell, D. B.; Sheppard, N.; Skinner, P. *J. Chem. Soc., Faraday Trans. 2* **1981**, *77*, 397.
(7) Dimas, P. A.; Duesler, E. N.; Lawson, R. J.; Shapley, J. R. *J. Am. Chem. Soc.* **1980**, *102*, 7787. Hermann, W. A.; Plank, J.; Riedel, D.; Ziegler, M. L. *Ibid.* **1981**, *103*, 63. Kruppa, W.; Schmid, G. *J. Organomet. Chem.* **1980**, *202*, 379. Booth, B. L.; Casey, G. C. *Ibid.* **1979**, *178*, 371. Canty, A. J.; Johnson, B. F. G.; Lewis, J.; Norton, J. R. *J. Chem. Soc., Chem. Commun.* **1972**, 1331. Deeming, A. J.; Underhill, M. *J. Organomet. Chem.* **1972**, *42*, C60. Gladfelter, W. L.; Geoffroy, G. L. *Adv. Organomet. Chem.* **1980**, *18*, 207. Chetcuti, M.; Green, M.; Howard, J. A. K.; Jeffrey, J. C.; Mills, R. M.; Pain, G. N.; Porter, S. J.; Stone, F. G. A.; Wilson, A. A.; Woodward, P. *J. Chem. Soc., Chem. Commun.* **1980**, 1057. Váradi, G.; Galamb, B.; Palágyi, J.; Pályi, G. *Inorg. Chim. Acta* **1981**, *53*, L29. Keister, J. B. *J. Chem. Soc., Chem. Commun.* **1979**, 214. Vahrenkamp, H. *Angew. Chem., Int. Ed. Engl.* **1978**, *17*, 379.
(8) Wong, K. S.; Fehlner, T. P. *J. Am. Chem. Soc.* **1981**, *103*, 966.
(9) Bau, R.; Teller, R. G.; Kirtley, S. W.; Koetzle, T. F. *Acc. Chem. Res.* **1979**, *12*, 176. Shaw, B. L. "Inorganic Hydrides"; Pergamon Press: New York, 1967. Bau, R., Ed.; "Transition Metal Hydrides"; American Chemical Society: Washington, D.C., 1978; Adv. Chem. Ser. No. 167.
(10) Teller, R. G.; Bau, R. *Struct. Bonding (Berlin)* **1981**, *44*, 1.

Table II. Selected Interatomic Distances (Å) and Angles (Deg) for $Fe_3(\mu\text{-}H)_3(CO)_9(\mu_3\text{-}CCH_3)$[a]

Distances			
Fe_1–Fe_2	2.617 (2)	C_{22}–O_{22}	1.131 (10)
Fe_1–Fe_3	2.618 (2)	C_{23}–O_{23}	1.137 (10)
Fe_2–Fe_3	2.619 (2)	C_{31}–O_{31}	1.139 (10)
Fe_1–C_{11}	1.781 (9)	C_{32}–O_{32}	1.133 (11)
Fe_1–C_{12}	1.825 (9)	C_{33}–O_{33}	1.127 (10)
Fe_1–C_{13}	1.777 (10)	Fe_1–C	1.946 (7)
Fe_2–C_{21}	1.744 (10)	Fe_2–C	1.947 (8)
Fe_2–C_{22}	1.815 (10)	Fe_3–C	1.948 (9)
Fe_2–C_{23}	1.794 (9)	C–CH_3	1.468 (14)
Fe_3–C_{31}	1.777 (9)	Fe_1–H_{12}	1.73 (7)
Fe_3–C_{32}	1.832 (12)	Fe_1–H_{13}	1.48 (7)
Fe_3–C_{33}	1.796 (9)	Fe_2–H_{12}	1.53 (7)
C_{11}–O_{11}	1.134 (9)	Fe_2–H_{23}	1.68 (7)
C_{12}–O_{12}	1.135 (9)	Fe_3–H_{13}	1.87 (7)
C_{13}–O_{13}	1.141 (10)	Fe_3–H_{23}	1.56 (7)
C_{21}–O_{21}	1.155 (10)		
Angles			
Fe_1–Fe_2–Fe_3	59.9 (0)	Fe_3–C_{32}–O_{32}	178.5 (10)
Fe_2–Fe_3–Fe_1	59.9 (0)	Fe_3–C_{33}–O_{33}	177.8 (8)
Fe_1–C–Fe_2	84.5 (3)	C_{11}–Fe_1–C_{12}	97.6 (4)
Fe_2–C–Fe_3	84.5 (3)	C_{12}–Fe_1–C_{13}	98.7 (4)
Fe_3–C–Fe_1	84.5 (3)	C_{13}–Fe_1–C_{11}	90.5 (4)
Fe_1–C–CH_3	129.7 (7)	C_{21}–Fe_2–C_{22}	96.9 (4)
Fe_2–C–CH_3	130.8 (7)	C_{22}–Fe_2–C_{23}	100.1 (4)
Fe_3–C–CH_3	126.6 (7)	C_{23}–Fe_2–C_{21}	90.9 (4)
Fe_1–C_{11}–O_{11}	179.3 (9)	C_{31}–Fe_3–C_{32}	99.8 (5)
Fe_1–C_{12}–O_{12}	177.5 (8)	C_{32}–Fe_3–C_{33}	97.3 (5)
Fe_1–C_{13}–O_{13}	177.6 (9)	C_{33}–Fe_3–C_{31}	90.3 (4)
Fe_2–C_{21}–O_{21}	178.1 (9)	Fe_1–H_{12}–Fe_2	106.7 (38)
Fe_2–C_{22}–O_{22}	178.9 (9)	Fe_2–H_{23}–Fe_3	107.6 (41)
Fe_2–C_{23}–O_{23}	179.8 (9)	Fe_3–H_{13}–Fe_1	102.1 (36)
Fe_3–C_{31}–O_{31}	179.2 (10)		

[a] The estimated standard deviations of the least significant digits are given in parentheses.

of main-group analogues[11] of I and II that allow investigation of the M–H–M interaction compared to the B–H–B interaction.[12] The succeeding paper[13] presents a detailed spectroscopic and theoretical analysis of the valence electron density distributions in I and II.

General Description of the Structure

The molecular structure of $Fe_3(\mu\text{-}H)_3(CO)_9(\mu_3\text{-}CCH_3)$ and the numbering system used are shown in Figures 1 and 2. The structural data are given in Tables I–III. The cluster core of II consists of an equilateral triangular framework of iron atoms with a methylidyne carbon 1.23 Å above the metal plane and on the threefold axis. Each iron is formally six-coordinate with three carbonyl carbon, two hydrogen, and one methylidyne carbon nearest neighbors. The methylidyne carbon contains a methyl substituent, also on the threefold axis, and is formally four-coordinate. Each edge of the metal triangle is bridged with a hydrogen atom that (within experimental error) is symmetrically placed and lies in the plane defined by the two bridged iron atoms and the methylidyne carbon (Table III). The entire molecule has C_{3v} symmetry, and the threefold axis is clearly revealed in Figure 2.

The distances and angles (Table II) are within ranges expected on the basis of the structure of similar compounds.[14] Specifically, the average Fe–Fe distance is 2.618 Å, the average Fe–C(apical) distance is 1.947 Å, the average Fe–C-(axial carbonyl) distance is 1.825 Å, the average Fe–C-(equatorial carbonyl) distance is 1.778 Å, the average C–O distance is 1.137 Å, and the average Fe–C–O angle is close to 180°. The average Fe–H distance is 1.64 Å, which is within the estimated standard deviation expected for X-ray determinations,[15] and the average Fe–H–Fe angle is 105.5°. When

Table III. Selected Molecular Planes in $Fe_3(\mu\text{-}H)_3(CO)_9(\mu_3\text{-}CCH_3)$

atom	dev, Å	atom	dev, Å
Plane 1: Fe_1, Fe_2, Fe_3			
$-0.3688X - 0.0684Y - 0.9269Z = -8.2042$			
Plane 2: Fe_1, C_{11}, C_{13}			
$-0.7733X + 0.3539Y - 0.5260Z = -1.6352$			
Plane 3: Fe_2, C_{21}, C_{23}			
$-0.3885X - 0.6967Y - 0.6030Z = -10.1984$			
Plane 4: Fe_3, C_{31}, C_{33}			
$0.3455X + 0.1588Y - 0.9248Z = -9.6052$			
Plane 5: Fe_1, C, Fe_2, H_{12}			
$0.5675X + 0.2070Y - 0.7968Z = -6.9724$			
Fe_1	−0.0082	C	0.0069
Fe_2	−0.0091	H_{12}	0.010
Plane 6: Fe_2, C, Fe_3, H_{23}			
$-0.7795X + 0.5380Y - 0.3207Z = 3.1599$			
Fe_2	0.0216	C	−0.0179
Fe_3	0.0232	H_{23}	−0.0270
Plane 7: Fe_3, C, Fe_1, H_{13}			
$-0.3597X - 0.8578Y - 0.3669Z = -7.4566$			
Fe_3	0.0056	C	−0.0053
Fe_1	0.0071	H_{13}	−0.0074
Plane 8: C_{11}, C_{13}, H_{12}, H_{13}			
$-0.7977X + 0.3589Y - 0.4844Z = -1.2481$			
Fe_1	−0.0539	Fe_2	−1.4972
Fe_3	−1.7354	C_{12}	1.7156
C_{11}	−0.0341	H_{12}	−0.0351
C_{13}	0.0296	H_{13}	0.0396
Plane 9: C_{21}, C_{23}, H_{12}, H_{23}			
$-0.3688X - 0.7123Y - 0.5970Z = -10.3355$			
Plane 10: C_{31}, C_{33}, H_{23}, H_{13}			
$0.3204X + 0.1708Y - 0.9317Z = -9.4765$			

planes	dihedral angle, deg	planes	dihedral angle, deg
1, 2	41.5	6, 7	86.4
1, 3	41.4	1, 8	44.0
1, 4	44.0	1, 9	42.4
5, 6	85.7	1, 10	42.8
5, 7	84.9		

Table IV. Comparison of Selected Geometrical Parameters for $Fe_3(\mu\text{-}H)_3(CO)_9(\mu_3\text{-}CCH_3)$ and $Co_3(CO)_9(\mu_3\text{-}CCH_3)$

parameters[b]	$Fe_3(H)_3(CO)_9CCH_3$	$Co_3(CO)_9CCH_3$[a]
$\angle(CO)_e$–M–$(CO)_e$, deg	90	97
$d_{M\text{-}M}$, Å	2.62	2.47
α,[b] deg	42	29
$d_{M\text{-}Cap}$, Å	1.95	1.90
β,[b] deg	50.9	48.6
$d_{Cap\text{-}CH_3}$, Å	1.468 (14)	1.53 (2.8)

[a] See ref 2. [b] See Figure 3 for designations.

(11) Wade, K. *Adv. Inorg. Chem. Radiochem.* **1976**, *18*, 1. Mingos, D. M. P. *J. Chem. Soc., Dalton Trans.* **1974**, 133.
(12) Lipscomb, W. N. "Boron Hydrides"; W. A. Benjamin: New York, 1963.
(13) DeKock, R. L.; Wong, K. S.; Fehlner, T. P. *Inorg. Chem.*, companion paper in this issue.
(14) Chini, P.; Heaton, B. T. *Top. Curr. Chem.* **1977**, *71*, 1.
(15) The X-ray method tends to give shorter M–H distances than neutron diffraction. See, for example: Petersen, J. L.; Williams, J. M. *Inorg. Chem.* **1978**, *17*, 1308.

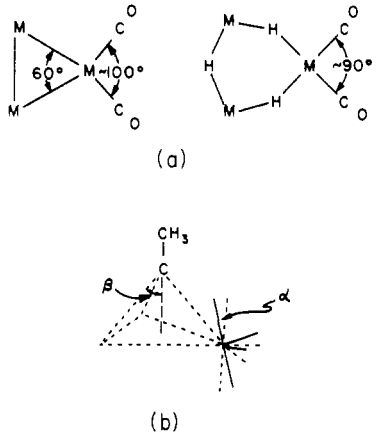

Figure 3. Relative orientation of CO ligands in clusters containing a metal triangle: (a) metal plane for $M_3(CO)_{12}$ and $M_3H_3(CO)_{12}$ showing two equatorial CO ligands; (b) $M_3(CO)_9CCH_3$ system defining the orientation of the metal octahedral bond vectors with respect to the metal plane.

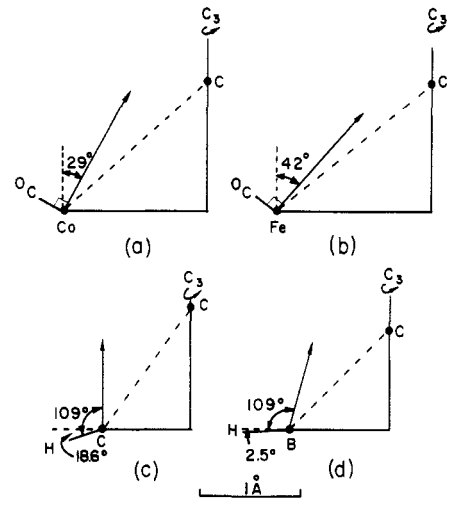

Figure 4. Cut of the M_3C and M'_3C tetrahedra containing the threefold axis: (a) M = Co; (b) M = Fe; (c) M′ = C; (d) M′ = B. Drawings are to the scale indicated.

the differences between Fe and Ru are taken into account, the observed geometrical parameters of II also agree well with those already published for $Ru_3(\mu\text{-}H)_3(CO)_9(\mu_3\text{-}CCH_3)$.[16]

Geometrical Comparison of the Cobalt and Iron Analogues

The solid-state structure of I (X = CH_3) has been reported and thoroughly discussed earlier by Sutton and Dahl.[3] A comparison of structural parameters with those found for II may be found in Table IV. The focus of this comparison is on the differences caused by the presence of bridging hydrogens in II. The primary differences are evidenced by the positioning of the exo-cluster ligands of the metal and the metal–metal distance. For a fuller appreciation of the meaning of these differences, the situation in uncapped triangular metal clusters is briefly reviewed.[17]

In equilateral triangular metal clusters formed from $M(CO)_4$ fragments (Figure 3) the environment of M is approximately octahedral. However, the $(CO)_e$–M–$(CO)_e$ angle is larger than 90° (about 100°), reflecting, as it were, the M–M–M angle of 60°. Going to the isoelectronic $H_3M_3(CO)_{12}$ system with three hydrogens symmetrically bridging the metal atoms results in two significant changes. The M–M distance increases by about 0.2 Å, and the $(CO)_e$–M–$(CO)_e$ angle decreases about 10–15°.[17] These two changes may be interpreted in terms of the bridging hydrogens acting as ligands; i.e., the hydrogen occupies space in a distinct metal coordination position such that a characteristic M–H distance is achieved. Proceeding now to the metal triangle of the CM_3 compounds, one finds that in going from I to II the M–M distance increases by 0.15 Å and the $(CO)_e$–M–$(CO)_e$ angle decreases from 97 to 90°. Thus, as far as the metal triangle is concerned, the situation is the same as that described for the uncapped M_3 system above and the bridging hydrogens may be said to be acting as ligands with respect to the metal.

The major difference between the M_3 and CM_3 systems is the fact that the approximate octahedral geometry of the metal as defined by the exo-cluster CO ligands is tilted in the latter case by an angle α (Figure 3) such that one octahedral bond vector points more toward the apical carbon. This tilt, which is present in both I and II, requires that bridging hydrogens behaving as ligands be found out of the M_3 plane on the side opposite the apical carbon. In fact, this is where they are observed for II. In addition, for II it will be noted from Table IV that the dihedral angle between the Fe_3 triangle and the plane defined by $(CO)_e$–Fe–$(CO)_e$ is 13° more than that for the cobalt[18] compound. This additional tilting is more than that required to accommodate the increase in the M–M distance caused by the bridging hydrogens in that the angle β defined in Figure 3 increases only 2.3°. This increased tilting in going from I to II may be ascribed to the necessity of attaining a characteristic Fe–H distance while retaining approximate octahedral geometry around the iron and a bonding interaction with the capping carbon atom. Thus, the bridging hydrogens in II are more than simply protons buried in the Fe–Fe bonds of $Fe_3(CO)_9CCH_3^{3-}$. They exhibit observable effects on geometry that are understandable in terms of the behavior expected of ligands.

The increased tilt of the metal octahedral bond vector toward the capping carbon in II compared to that in I suggests a significant perturbation of the bonding of the capping carbon to the triangular metal base. In Figure 4 a cut containing the threefold axis and one metal atom is shown for I and II. The idealized octahedral bond vectors pointing toward the capping carbon are shown, and it may be seen that this vector lies more closely to a line joining metal and carbon atoms for II than for I. This in turn suggests that the optimal hybridization for the capping carbon may be different in the two compounds. Such a difference might be expected to be experimentally reflected in the C–C bond length between the capping carbon and the methyl substituent. Although the value found for this distance is smaller for II than for I, the difference is not statistically significant. Despite this lack of experimental verification, this analysis suggests that the bonding requirements of the bridging hydrogens acting as ligands induce a change in the bonding environment of the capping carbon atom that may well be reflected in its other properties, e.g., chemistry.

Geometrical Comparison of Analogous Model Compounds

The analogy between the bonding properties of certain main-group fragments and transition-metal fragments is an established concept of proven utility in the analysis of the bonding in metal systems.[11] That is, the formal substitution of an isolobal, pseudoisoelectronic main-group fragment for a transition-metal fragment often allows a simple analysis of the major interactions in an ostensibly complex system. As $Co(CO)_3 \approx C\text{–}H$ and $Fe(CO)_3 \approx B\text{–}H$ the main-group ana-

(16) Sheldrick, G. M.; Yesinowski, J. P. *J. Chem. Soc., Dalton Trans.* **1975**, 873.

(17) For a more complete discussion and leading references, see: Kaesz, H. D. *J. Organomet. Chem.* **1980**, *200*, 145.

(18) Using the axial CO's for reference yields approximately the same increase in tilting in going from I to II.

Table V. Comparison of Selected Optimized Geometrical Parameters for $CH_3C_4H_3$ and $CH_3CB_3H_6$

parameters	$CH_3CB_3H_6$	$CH_3C_4H_3$
d_{C-C}, d_{B-B}, Å	1.876	1.491
α, deg	−2.5	−18.6
$d_{C-C_{ap}}$, $d_{B-C_{ap}}$, Å	1.547	1.525
β, deg	44.5	35.7
d_{C-CH_3}(III), d_{C-CH_3}(IV), Å	1.517	1.506

logues of I and II are $(CH_3)CC_3H_3$ (III) and $(CH_3)CB_3H_6$ (IV). The first, methyl-substituted tetrahedrane, has been

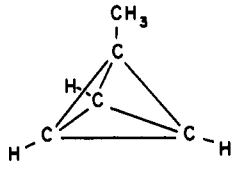

III

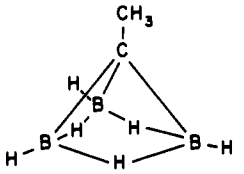

IV

isolated as another substituted derivative[19] and has been the subject of spectroscopic and theoretical effort.[20] The isoelectronic compound IV is presently unknown but has the structure indicated. It occurred to us that, as presently available theoretical methods provide the ability to accurately "determine" the structures of relatively small (in terms of electrons) systems, it would be useful to compare the geometrical changes in going from III to IV with those observed in going from I to II. This comparison should demonstrate whether the main-group analogues do in fact provide an adequate description of the bonding in the metal clusters insofar as bonding is expressed in geometry.

To obtain the geometries of III and IV, we carried out ab initio molecular orbital calculations as indicated below. Similar calculations were carried out on the unsubstituted molecules, C_4H_4 and HCB_3H_6, and the calculated structure, energy, and eigenvalues of the former agree well with those previously reported.[20] Selected geometrical parameters for III and IV are given in Table V and are organized in a fashion similar to those for I and II in Table IV.

In comparing the M'_3 triangle (M′ = C or B), one finds an increase in the M′–M′ distance of 0.38 Å in going from III to IV which is in the same direction but twice as large as that for I to II. The M′ atoms have approximately tetrahedral geometry whose orientation is defined by the M′–H bond vector. This is shown in Figure 4, where a cut containing the threefold axis and one M′ atom is displayed. The angle the M′–H bond vector makes with the M'_3 plane changes by 16° in going from III to IV, the direction of the change being the same as for I to II. The idealized tetrahedral bond vector pointing toward the apical carbon lies more closely to a line joining M′ and C for IV than for III. Just as for the metal compounds, this increased tilting in going from III to IV may be ascribed to a manifestation of the ligand character of the bridging hydrogens. As the increase in M′–M′ distance and increase in tilting are the only two significant changes[21] observed in going from III to IV, and as the relative changes parallel those in going from I to II, one concludes that the model compounds do indeed reflect the principal cluster bonding interactions as perturbed by the presence of cluster bridging hydrogens. It is significant to note that the bridging hydrogen is only 0.02 Å out of the B–C–B plane in IV, which is analogous to the situation in II. At this level then, the Fe–H–Fe bonds of II may be considered to be analogous to the B–H–B bonds of IV, i.e., open three-centered two-electron bonds.

Table VI. Mulliken Overlap Populations for Bonds in C_4H_4, HCB_3H_6, $(CH_3)C_4H_3$, and $(CH_3)CB_3H_6$[a]

bonds[b]	C_4H_4	HCB_3H_6	$(CH_3)C_4H_3$	$(CH_3)CB_3H_6$
$M'-H_T$	0.79	0.81	0.78	0.81
M′–M′	0.51	0.10	0.50	0.10
$B-H_{Br}$		0.39		0.38
$M'-C_{ap}$	0.51	0.71	0.51	0.70
$C_{ap}-H$	0.79	0.80		
$C_{ap}-C_{Me}$			0.75	0.75

[a] STO-3G basis set only. [b] Abbreviations: T = terminal; Br = bridge; Me = methyl; ap = apical; M′ = B or C basal.

Table VII. Mulliken Charge Analysis (Net Atomic Charges) for the Apical Carbon and Hydrogen for C_4H_4 and HCB_3H_6

	C_4H_4		HCB_3H_6				
basis set	C	H	C	H_C	B	H_{Br}	H_T
STO-3G	0.10−	0.10+	0.32−	0.08+	0.14+	0.05−	0.02−
4-31G	0.21−	0.21+	0.64−	0.21+	0.08+	0.03+	0.04+
6-31G	0.23−	0.23+	0.55−	0.23+	0.04+	0.02+	0.05+

Just as the different orientations of the metal coordination bond vectors in I and II suggest different bonding environments for the capping carbon, so too the different orientations of the M′ coordination bond vectors in III and IV suggest a perturbation in the bonding of the capping carbon. The quantum chemical calculations allow this point to be more fully explored, and in Table VI selected results of a Mulliken population analysis for III and IV are compared. First, there is no significant difference between the net overlap population in the capping carbon–methyl carbon bond in III and IV. In fact, there is no real change in any of the exo-cluster bonds. However, there are substantial changes within the cluster. When one goes from III to IV, the direct M′–M′ bonding is nearly eliminated and replaced by M′–H–M′ bonding, i.e., an open three-center bond. The M′–capping carbon interaction remains large in going from III to IV, indicating little change despite a large M′–M′ distance increase. This is reflected in the similarity of the M′–C distances (Table IV). It seems, then, that the increased tilting of the M′ tetrahedral geometry required to accommodate the bridging hydrogen in going from III to IV is also consonant with retention of a strong M′–capping carbon interaction.

A charge analysis (i.e., net atomic charges from Mulliken population analysis) for C_4H_4 and HCB_3H_6 is given in Table VII for the three basis sets used. The absolute charges depend on the basis set, but the relative charges and the changes from III to IV are the same. There is a large difference in the net charges of the capping carbons, that of IV being much more negative. Comparison of the numbers averaged for the three calculations demonstrates that, when M′ goes from C to B, M′ loses 1.27 electrons of which 0.16 end up on the M′–H terminal hydrogen, 1.00 on the bridging hydrogens, and 0.11 on the capping carbons. As there are three M′ atoms, the electronic charge of the capping carbon increases by 0.33 electron. Thus, the capping carbon is indeed very different in IV compared to that in III but the difference is most easily explained in terms of the relative electronegativities of M′. Thus, the calculations demonstrate greater polarization of charge in IV vs. that in III but little evidence for any essential changes in the bonding between capped carbon and the M'_3 triangle.[22] It seems that the increased tilt in IV relative to

(19) Maier, G.; Pfriem, S.; Schaefer, U.; Matusch, R. *Angew. Chem., Int. Ed. Engl.* **1978**, *17*, 520.
(20) Heilbronner, E.; Jones, T. B.; Krebs, A.; Maier, G.; Malsch, K.; Pocklington, J.; Schmelzer, A. *J. Am. Chem. Soc.* **1980**, *102*, 564.
(21) The $C_{ap}-C_{Me}$ changes by 0.12 Å and the $M'-C_{ap}$ changes by 0.022 Å.
(22) The polarization of charge is reflected in the calculated dipole moments, which are 0.31 and −0.68 D (in the direction of the C_3 axis) in III and IV, respectively.

that in III serves to compensate for the increased M'–M' distance and the net bonding interaction is about the same.

Experimental Section

Synthesis and Characterization. All reactions and manipulations were carried out under inert atmospheres or in a vacuum line with use of standard techniques.[23] Infrared spectra were obtained on a Perkin-Elmer 727B, ^1H and ^{13}C NMR spectra were obtained on Varian XL-100 and Nicolet NB-300 instruments, and mass spectra were recorded on AEI-MS 9 and Du Pont DP-1 GC/MS instruments. Commercially available $Fe(CO)_5$ was used without further purification, and solvents were distilled from benzophenone ketyl under N_2 before use. $Na_2Fe_2(CO)_8$ was prepared as described elsewhere.[24]

Reactions of $Na_2Fe_2(CO)_8$ with BH_3/THF (1:2 molar ratio) under vacuum (or inert atmosphere) for about 5–10 h followed by acidification with a slight excess of concentrated H_2SO_4 were performed in a 500-mL thick-wall round-bottom flask equipped with an O-ring stopcock.[25] After acidification, noncondensible gases (believed to be CO and H_2) were removed. After removal of solvents under vacuum, the alkylidynetriiron species were the only volatile products collected. The yield of II is about 10–20%. The compound is volatile enough to handle in a standard vacuum line and is readily soluble in a wide range of organic solvents. It is a brown solid at room temperature and decomposes slowly in air.

Spectra. The solution infrared spectrum of II (hexane, CaF_2 cells) shows peaks in the CO stretching region at 2075 (s), 2040 (s), and 2015 (m) cm^{-1}. The highest peak observed in the mass spectrum has $m/e = 450$ and is assigned as the parent ion. The 100-MHz ^1H FT NMR spectrum of II in toluene at ambient temperature exhibits a singlet characteristic of metal hydrides at δ −23.6 and a singlet at δ 4.3 assigned to the methyl protons. The 25.2-MHz ^{13}C FT NMR[26] in toluene exhibits a broadened singlet at 206 ppm, which is assigned to the carbonyl ligands bound to iron.[27] A single peak at 45.7 ppm is also observed, and this is assigned to the methyl carbon. No resonance attributable to the quaternary carbon could be detected.[28]

X-ray Crystallographic Data. A single crystal of II, 0.3 × 0.4 × 0.07 mm^3 was formed from the gas phase by slow cooling of a pure sample. The crystal was mounted in a capillary under nitrogen and was determined to be triclinic (space group $P\bar{1}$) with a = 7.979 (2) Å, b = 9.478 (3) Å, c = 12.714 (4) Å, α = 93.45 (3)°, β = 106.94 (3)°, and γ = 60.79 (3)°. The unit cell volume of 799 $Å^3$ led to a calculated density of 1.87 g cm^{-3} for two molecules of II in the unit cell.

X-ray intensity data were collected at 292 K on a Syntex $P\bar{1}$ diffractometer equipped with a graphite-monochromated Mo Kα radiation source by using θ–2θ scan techniques, with scan speeds varying from 2 to 12° min^{-1}, to the limit $2\theta < 55°$. The intensities of four standard reflections, monitored at regular intervals, showed no significant fluctuation during the collection procedure. The raw intensity data were corrected for Lorentz and polarization effects; however, no absorption correction was applied [μ(Mo Kα) = 27.3 cm^{-1}]. After equivalent reflections were averaged, a total of 2496 independent reflections were used for solution and refinement.

The iron atoms were located by direct methods with use of the MULTAN[29] package. The rest of the non-hydrogen atoms were located by Fourier techniques, and the model was refined to convergence by assuming anisotropic vibration of the atoms. The bridging hydrogen atoms were located from a difference electron density map and included in the model as isotropic atoms. Full-matrix least-squares refinement was based on minimization of the function $\sum w(|F_o| - |F_c|)^2$ with the weights w taken as $(2F_o/\sigma F_o^2)^2$, where F_o and F_c are the observed and calculated structure factor amplitudes, respectively. Atomic scattering factors for non-hydrogen atoms were taken from Cromer and Waber.[30] The final agreement factors are R_1 = 0.076 and R_2 = 0.075,[31] and the estimated standard deviation of an observation of unit weight is 1.93. The ratio of data to parameters is 11.3. Atomic coordinates and thermal parameters for all atoms are listed in Table I. Interatomic distances and angles and deviations of atoms from selected planes are listed in Tables II and III, respectively.

Quantum Chemical Calculations. Ab initio molecular orbital calculations were carried out with use of a modified version of GAUSSIAN 70 with an STO-3G basis set.[32] All molecular geometries were optimized completely, subject only to overall molecular symmetry constraints. The changes in bond lengths and angles upon a second cycle of optimization were negligible. Geometry optimization of HCB_3H_6 with a larger basis set (4-31G) also produced negligible change with respect to the STO-3G results. Single-point calculations at the STO-3G optimized geometries were carried out with more flexible basis sets (4-31G and 6-31G),[33] and the latter lead to essentially the same conclusions as the STO-3G calculations.

Acknowledgment. The support of the National Science Foundation (Grant No. CHE 78-11600) is gratefully acknowledged (K.S.W., T.K.D., and T.P.F.). This research was also supported in part by the Office of Basic Energy Sciences of the Department of Energy (D.M.C.). T.K.D. acknowledges a grant from the Graduate Student Union at Notre Dame. This is Document No. NDRL-2301 from the Notre Dame Radiation Laboratory. We thank the University of Notre Dame Computing Center for providing computing time and Professor W. R. Scheidt for providing aid in the crystal structure determination. The 300-MHz NMR was purchased with the support of the National Institutes of Health (Grant No. GM 25845-02S1).

Registry No. I, 13682-04-7; II, 69440-00-2; III, 22907-84-2; IV, 81940-44-5; C_4H_4, 157-39-1; HCB_3H_6, 81940-45-6.

Supplementary Material Available: A listing of observed and calculated structure factor amplitudes (9 pages). Ordering information is given on any current masthead page.

(23) Shriver, D. F. "The Manipulation of Air-Sensitive Compounds"; McGraw-Hill: New York, 1969.
(24) Collman, J. P. *Acc. Chem. Res.* **1975**, *8*, 342.
(25) This is an improved preparation over that reported earlier.[8]
(26) The sample for ^{13}C NMR study was prepared with about 30% ^{13}C enrichment. A 75.5-MHz FT NMR spectrum is characterized by fine structure on each of the observed signals. This structure can be considered as the ^{57}Fe satellite subspectrum, which appears as doublets with an inner separation of 32–35 Hz. See: Aime, S.; Oscella, D. *J. Organomet. Chem.* **1981**, *214*, C27.
(27) Iron carbonyl shifts are typically observed in the range 210–220 ppm. Todd, L. J.; Wilkinson, J. R. *J. Organomet. Chem.* **1974**, *77*, 1.
(28) A resonance for the quaternary carbon was not reported for $H_3Ru_3(CO)_9CCH_3$. Canty, A. J.; Johnson, B. F. G.; Lewis, J.; Norton, J. R. *J. Chem. Soc., Chem. Commun.* **1972**, 1331.
(29) Germain, G.; Main, P.; Woolfson, M. M. *Acta Crystallogr., Sect. A* **1971**, *A27*, 368. Other programs used as well as a description of data collection and data reduction methods can be found in: Scheidt, W. R. *J. Am. Chem. Soc.* **1974**, *96*, 84.
(30) Cromer, D. T.; Waber, J. T. "International Tables for X-ray Crystallography"; Kynoch Press: Birmingham, England, 1974; Vol. 4.
(31) $R_1 = \sum(|F_o| - |F_c|)/\sum|F_o|$; $R_2 = [\sum w(|F_o| - |F_c|)^2/\sum w|F_o|^2]^{1/2}$.
(32) Hehre, W. J.; Stewart, R. F.; Pople, J. A. *J. Chem. Phys.* **1969**, *51*, 2657. Hehre, W. J.; Ditchfield, R.; Pople, J. A. *Ibid.* **1970**, *52*, 2191. Ditchfield, R.; Hehre, W. J.; Pople, J. A. *Ibid.* **1971**, *54*, 724. Hehre, W. J.; Lathan, W. A. *Ibid.* **1972**, *56*, 5255. Hehre, W. J.; Lathan, W. A.; Ditchfield, R.; Newton, M. D.; Pople, J. A. *QCPE* **1973**, *11*, 236.
(33) Binkley, J. S.; Whiteside, R. A.; Hariharon, P. C.; Seeger, R.; Pople, J. A.; Hehre, W. J.; Newton, M. D. *QCPE* **1978**, *11*, 368.